Mol Neurobiol (2014) 49:1472–1486
DOI 10.1007/s12035-014-8650-8

Epigenetic Modulation of Adult Hippocampal Neurogenesis by Extremely Low-Frequency Electromagnetic Fields

Lucia Leone · Salvatore Fusco · Alessia Mastrodonato · Roberto Piacentini · Saviana Antonella Barbati · Salvatore Zaffina · Giovambattista Pani · Maria Vittoria Podda · Claudio Grassi

Received: 31 July 2013 / Accepted: 22 January 2014 / Published online: 16 February 2014
© Springer Science+Business Media New York 2014

Abstract Throughout life, adult neurogenesis generates new neurons in the dentate gyrus of hippocampus that have a critical role in memory formation. Strategies able to stimulate this endogenous process have raised considerable interest because of their potential use to treat neurological disorders entailing cognitive impairment. We previously reported that mice exposed to extremely low-frequency electromagnetic fields (ELFEFs) showed increased hippocampal neurogenesis. Here, we demonstrate that the ELFEF-dependent enhancement of hippocampal neurogenesis improves spatial learning and memory. To gain insights on the molecular mechanisms underlying ELFEFs' effects, we extended our studies to an in vitro model of neural stem cells (NSCs) isolated from the hippocampi of newborn mice. We found that ELFEFs enhanced proliferation and neuronal differentiation of hippocampal NSCs by regulation of epigenetic mechanisms leading to pro-neuronal gene expression. Upon ELFEF stimulation of NSCs, we observed a significant enhancement of expression of the pro-proliferative gene hairy enhancer of split 1 and the neuronal determination genes NeuroD1 and Neurogenin1. These events were preceded by increased acetylation of H3K9 and binding of the phosphorylated transcription factor cAMP response element-binding protein (CREB) on the regulatory sequence of these genes. Such ELFEF-dependent epigenetic modifications were prevented by the Ca_v1-channel blocker nifedipine, and were associated with increased occupancy of CREB-binding protein (CBP) to the same loci within the analyzed promoters. Our results unravel the molecular mechanisms underlying the ELFEFs' ability to improve endogenous neurogenesis, pointing to histone acetylation–related chromatin remodeling as a critical determinant. These findings could pave the way to the development of novel therapeutic approaches in regenerative medicine.

Keywords Hippocampal neural stem cells · CREB · Ca_v1 channels · Epigenetics · Hes1 · NeuroD1 and Neurogenin1 modulation · Spatial memory

Introduction

Much experimental evidence has undoubtedly demonstrated that newborn neurons are continuously generated throughout life in several areas of the mammalian brain, especially in the subgranular zone (SGZ) of the hippocampal dentate gyrus (DG) [1]. Adult-generated granule cell neurons incorporate into hippocampal circuitry [2, 3] and are implicated in hippocampal functions including learning and memory [4–8]. Therefore, there is great interest in identifying stimuli able to preserve or enhance endogenous neurogenesis and ultimately improve hippocampal-mediated cognitive functions. Such approaches could be useful to counteract the diminished hippocampal neurogenesis and cognitive impairment occurring during normal aging and in several neurodegenerative diseases [9–11].

Lucia Leone and Salvatore Fusco equally contributed to this work.

Electronic supplementary material The online version of this article (doi:10.1007/s12035-014-8650-8) contains supplementary material, which is available to authorized users.

L. Leone · S. Fusco · A. Mastrodonato · R. Piacentini · S. A. Barbati · M. V. Podda · C. Grassi (✉)
Institute of Human Physiology, Medical School, Università Cattolica, Largo Francesco Vito 1, 00168 Rome, Italy
e-mail: grassi@rm.unicatt.it

S. Zaffina
Children's Hospital "Bambino Gesù", Rome, Italy

G. Pani
Institute of General Pathology, Medical School, Università Cattolica, Rome, Italy

In recent years, a variety of physiological, environmental and pharmacological stimuli affecting adult hippocampal neurogenesis have been identified [12–14]. Physical stimuli, such as electromagnetic fields, have also been proved to effectively modulate endogenous neurogenesis [15–20]. In particular, we previously reported that exposure to ELFEFs (1 mT, 50 Hz) enhances adult hippocampal neurogenesis and promotes newborn neuron survival in vivo [16, 17]. The surviving newborn cells mainly differentiate into granule neurons and are functionally integrated into the dentate network, enhancing synaptic plasticity [17].

The signaling cascades that finely tune and coordinate this process in the adult brain have been poorly investigated and remain largely unknown. The neurogenic process is known to rely on the activation of specific and complex transcriptional programs involving the basic helix–loop–helix (bHLH) transcription factors, finally resulting in the expression of a cascade of neuronal genes [21–23]. The bHLH gene family includes the repressor-type hairy enhancer of split 1 (Hes1), which keeps constant the NSC reservoir [24], and the activator-type genes Mash1, Neurogenin1 and NeuroD1 that are strongly associated with the pan-neuronal gene expression and the neuronal fate determination [25–28].

Compelling evidence shows that specific gene expression programs are, in part, orchestrated by epigenetic mechanisms. In particular, chromatin remodeling via histone modifications at gene promoter regions is a key mechanism controlling gene expression. According to the "histone code theory", histone acetylation/deacetylation at a particular promoter region defines a specific epigenetic state that encodes gene activation vs. gene silencing [29]. Intriguing correlations have been found between the balance of histone acetylation/deacetylation at particular promoter regions and the correct activation and/or inactivation of neurogenic programs [30–33]. Several lines of evidence suggest that the level of histone H3 and H4 acetylation is highly dynamic during the development of the nervous system and neuronal nucleosome assembly can affect neurogenesis and neurodifferentiation [34, 35]. It is worth noting that these epigenetic modifications have recently been implicated in memory formation [36–40] and their malfunction can contribute to the pathogenesis of cognitive disorders [41, 42].

Here, we demonstrate that in mice exposed to ELFEFs enhanced hippocampal neurogenesis and synaptic plasticity lead to improved spatial learning and memory. From the molecular point of view the ELFEF-promoted enhancement of NSC proliferation and neuronal cell-fate specification is associated with increased histone H3 acetylation at lysine 9 (H3K9) and binding of both activated cAMP response element-binding protein (pCREB) and the transcriptional co-regulator CREB-binding protein (CBP) at the promoter of specific bHLH neuronal genes.

Materials and Methods

All experiments were conducted according to protocols reviewed and approved by the Ethics Committee of the Catholic University. Animals were housed and handled in accordance with European Community guidelines (Council Directive 86/609/EEC of 24/11/1986). Unless otherwise specified, all commercial products were used according to manufacturers' instructions.

Exposure to ELFEFs

In vivo experiments were performed on 38 adult male C57bl/6 mice (4–5 weeks old) that were randomly divided into two groups: (1) sham-exposed animals (controls) and (2) ELFEF-exposed mice.

ELFEF stimulation (1 mT; 50 Hz; 3.5 h/day for 12 days (12D×3.5 h)) was delivered by means of a solenoid generating alternating EFs characterized by a sinusoidal waveform with amplitudes of 5–1,000 μT and frequencies of 1–100 Hz. This device was supplied by a power generator, and EF frequency and amplitude were monitored by an EF sensor connected to a digital multimeter and oscilloscope [16–20]. The stimulation intensity was chosen based on our previous studies showing that 1 mT ELFEF stimulation produced maximum effects on cell fate in neuroendocrine cells [43] and significantly enhanced in vivo adult hippocampal neurogenesis [16]. The solenoid was made of copper wire wrapped around a Plexiglas cylinder (diameter 20 cm; length 42 cm) with open extremities in which the plastic cage containing freely moving animals (3–4 mice in each cage) was positioned. The geometry of the system assured field uniformity within the entire length of the cage that was of the same size of that used for the normal housing of the mice (i.e., 33×15×13 cm). The force lines of the alternating EFs in the solenoid were almost parallel to the animal longitudinal head-to-tail axis.

Control mice were placed inside the chamber for the same amount of time as their exposed counterparts, but the generator supplying the solenoid was turned off (sham exposure). Great care was taken to avoid any stress and animal discomfort. Animals of both groups never showed unusual behaviors during and after exposure.

For in vitro experiments, NSCs, isolated as described hereafter, were continuously exposed to ELFEFs produced by the same device used for in vivo experiments with the solenoid being placed inside the CO_2 incubator [20, 43, 44]. The surfaces of the culture well plates were parallel to the force lines of the alternating magnetic field in the solenoid. Control cells were grown in a different CO_2 incubator. Air and culture-medium temperatures were continuously monitored for the

duration of experiments with thermometric probes (Homeometric Control Unit, Harvard Apparatus Ltd., Edenbridge, UK; 0.1 °C accuracy). The maximum temperature increase recorded in the cultures exposed to ELFEFs (compared with unexposed cultures) was 0.4±0.1 °C. To identify the possible influence of this modest increase in temperature on our results, we compared data obtained from NSCs cultured in two different CO_2 incubators at temperature settings of 37.0 and 37.4 °C. No significant changes in the studied parameters were observed.

As described in Fig. 1, different exposure times were used to assess the effects of ELFEFs (1 mT; 50 Hz) (a) in vivo, on behavior testing, fate and integration of newborn neurons in the granular cell layer (GCL; 3.5 h/day for 12 days (12D× 3.5 h); Fig. 1a); (b) in vitro, on the expression of specific genes and proteins (24 h/day for 2 days (2D×24 h); Fig. 1b).

Morris Water Maze

Spatial learning and memory were assessed using the Morris water maze (MWM) test on control (n=14) and ELFEF-exposed mice (n=16) [17, 45]. Briefly, the experimental apparatus consisted of a circular plastic pool (127 cm in diameter) filled with water colored with nontoxic white paint to obscure the location of a submerged platform. The pool was ideally divided into four equal quadrants (NE, corresponding to the target quadrant, SE, NW, and SW) and the platform (10×10 cm) was placed at the center of the target quadrant in a fixed position. Visual cues were placed on the walls around the pool to orient the mice. The acquisition training session was performed 4 days before the test session (probe test) and consisted of six trials a day for four consecutive days, during which the animals were allowed to reach the platform within

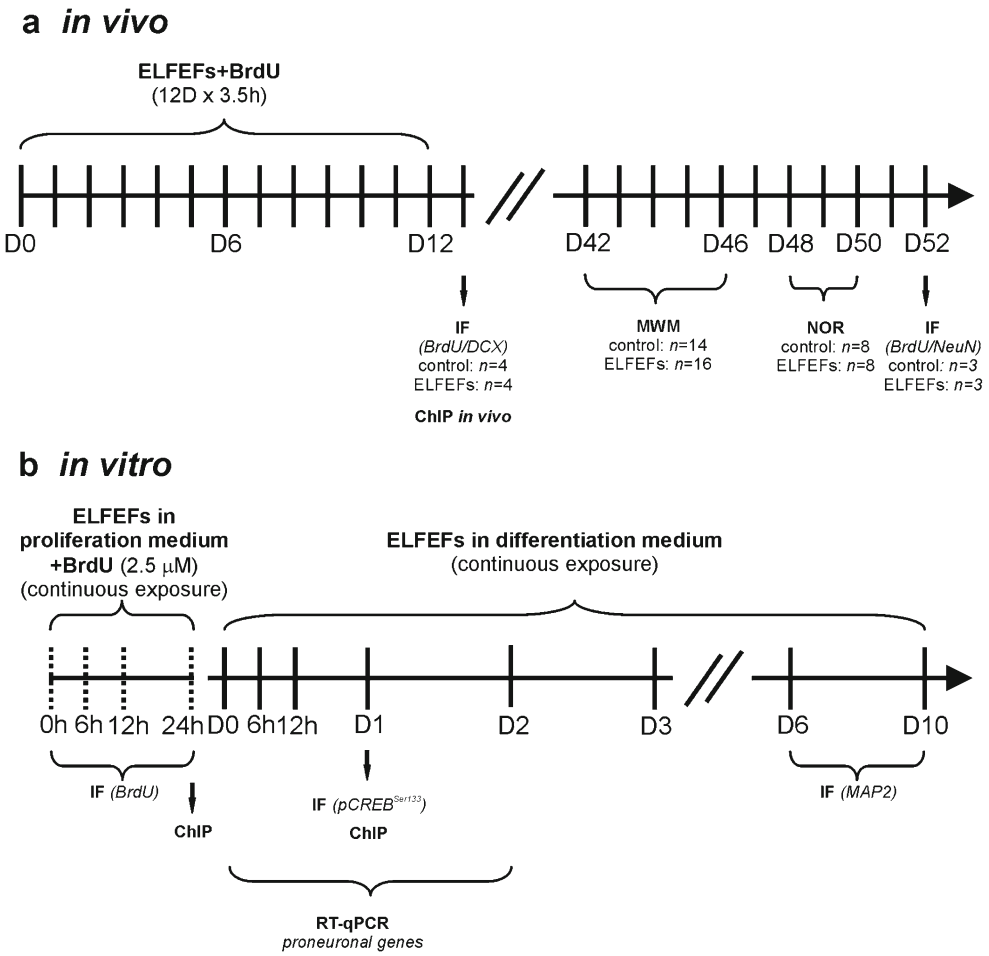


Fig. 1 Schematic representation of the experimental design and time schedule of the protocol. **a** Thirty-eight adult male C57bl/6 mice underwent ELFEFs (n=20) and sham exposure (n=18) for 12 days and were daily injected with 5-bromo-2′-deoxyuridine (*BrdU*; 100 mg/kg). A first group of mice was killed soon after treatment for immunofluorescence and chromatin immunoprecipitation experiments. A second group of animals was subjected to behavioral tests and killed 40 days after the end of the treatment for immunofluorescence analysis. **b** Adult hippocampal neural stem cells (*NSCs*) cultured in proliferation (time course from 0 to 24 h) and differentiation media (time course from 0 to 10 days) were continuously exposed to ELFEFs or left in control conditions and subsequently processed for immunocytochemical and molecular analyses. *ELFEFs,* extremely low-frequency electromagnetic fields; *IF*, immunofluorescence; *ChIP*, chromatin immunoprecipitation; *MWM*, Morris water Maze test; *NOR*, novel object recognition test

40 s. At the beginning of each trial, mice were immersed in the water, facing the wall, at one of three randomly assigned start positions (located in the quadrants not containing the platform). The starting points were varied daily. Time (latency) needed to navigate to the platform were recorded by an automated video tracking system (Panlab Harvard Apparatus).

Mice that failed to locate the platform in the allotted time were manually guided by the investigator. Mice were allowed to remain on the platform for 10 s and then returned to their home cages. The probe test session was performed 24 h after the last day of the training. In this session, the platform was removed from the pool and each mouse was allowed to swim for 60 s; the time spent in each quadrant was measured.

Novel Object Recognition

The general procedure consists of three consecutive days: a familiarization phase, a training phase and a test phase. On the 1st day, mice were individually submitted to a single familiarization session of 10 min, during which they were introduced into the empty arena (45×45 cm), in order to become familiar with the apparatus. On the 2nd day, animals were submitted to a single 10-min session (training phase) during which two identical objects were placed in a symmetric position from the center of the arena. An explorative behavior was scored when the head of the animal was facing close (less than 2 cm away) to the object or any part of the body except the tail was touching the object. The time spent exploring each object was recorded. The animals were returned to their home cages immediately after training. On the 3rd day, during the test phase, one of the familiar objects used during the training was replaced by a novel object and the animals were allowed to explore freely for 10 min. All objects were balanced in terms of physical complexity and were emotionally neutral. Moreover, the open-field and objects were thoroughly cleaned by 70 % alcohol after each session to avoid possible odorant cues. A preference index, a ratio of the amount of time spent exploring the novel object over the total time spent exploring both objects (during the retention session), was used to measure recognition memory.

BrdU Injection and Ex Vivo Immunofluorescence Assays

For 12 consecutive days, mice (n=7) were placed inside the solenoid for a daily ELFEF exposure of 3.5 h. Before each exposure, animals received an intraperitoneal injection of 5-bromo-2′-deoxyuridine (BrdU; 100 mg/kg dissolved in sterile 0.9 % NaCl solution; Sigma, Milan, Italy). Sham-exposed control animals (n=7) received the same treatment. Animals were sacrificed 24 h or 40 days after the final exposure session (D13 and D52 in Fig. 1a) to assess the effects of ELFEFs on the generation of immature and mature neurons, respectively. Mice were anesthetized with a cocktail of ketamine (100 mg/ml) and medetomidine (1 mg/ml) (ratio: 5:3) and transcardially perfused with an oxygenated Ringer's solution, pH 7.3, followed by 4 % freshly depolymerized paraformaldehyde in 0.1 M phosphate buffered saline (PBS), pH 7.4 [46]. The brain was removed from the skull, post-fixed overnight at 4 °C, and then transferred to a solution of 30 % sucrose in PBS for 2 days. Sagittal or coronal brain sections (45-μm-thick) were then cut with a vibratome (VT1000S, Leica Microsystems, GmbH, Wetzlar, Germany) and floated in ice-cold PBS. Sections were collected and stored until use in cryoprotectant at −20 °C [47, 48].

For assessment of BrdU incorporation, sections were incubated for 30 min in 2 N HCl at 37 °C to denature DNA, rinsed in PBS, and blocked for 45 min at room temperature (RT) in 1 % bovine serum albumin (BSA) solution containing 10 % goat serum and 0.5 % Triton X-100 (Sigma). The sections were then incubated for 48 h at 4 °C with the primary antibody (rat monoclonal anti-BrdU, 1:400; Abcam, Cambridge, UK), extensively washed, and then reincubated with the secondary antibody (AlexaFluor-488 anti-rat IgG, 1:600; Invitrogen, San Giuliano Milanese, Italy). For detection of doublecortin (DCX) expression, sections were incubated for 2 h with rabbit polyclonal anti-DCX antibody (1:200; Cell Signaling Technology Inc., Danvers, MA, USA), washed several times in PBS, and incubated with secondary antibodies (AlexaFluor-546 donkey anti-rabbit IgG, 1:500; Invitrogen). Cells were also double labeled with BrdU antibody (as described above) plus mouse monoclonal anti-NeuN antibody (1:150; Chemicon, Temecula, CA, USA). This marker was then visualized with Alexa-546 donkey anti-mouse (1:500 Invitrogen). Cell nuclei were counterstained with 4′6-diamidino-2-phenylindole (DAPI; 0.5 μg/ml; Invitrogen) and the sections were mounted on glass slides and cover-slipped with ProLong Gold antifade reagent (Invitrogen). We used the optical dissector method to estimate the number of labeled cells in the DG [49, 50]. Cells were counted under the 40× objective of an Olympus BX51 microscope (Tokyo, Japan) without any knowledge of the origin of the group. All labeled cells within each DG layer were counted separately in every sixth section throughout the entire hippocampus. The sum of these cell counts was then multiplied by 6 to estimate the total number of labeled cells within a given layer.

Images were obtained with a confocal laser scanning system (TCS-SP2, Leica Microsystems) equipped with an Ar/ArKr laser for 488-nm excitation and HeNe laser for 543-nm excitation. DAPI staining was imaged during two-photon excitation (740 nm, <140 fs, 90 MHz) performed with an ultrafast, tunable, mode-locked Ti: Sapphire laser (Chameleon, Coherent, Inc., Santa Clara, CA, USA). Ten- to fifteen-micrometer-thick confocal optical sections in hippocampal slices were analyzed.

Neural Stem Cell Culture

Postnatal hippocampal NSC culture were isolated according to previously published protocols [51]. Briefly, brains of newborn (0–1 day old) C57bl/6 mice were microdissected to obtain the hippocampal region upon sagittal sectioning. Tissues were finely minced and digested by accutase (in DPBS, 0.5 mM EDTA; Innovative Cell Tecnologies, Inc., San Diego, CA, USA) at 37 °C for 30 min. After centrifugation, cells were carefully dissociated by passaging in fire-polished Pasteur pipettes and resuspended in NeurobasalA medium, supplemented by 2 % B27 (Gibco, Grand Island, NY, USA), Glutamax (0.5 mM; Invitrogen, Carlsbad, CA), mouse fibroblast growth factor 2 (FGF2, 10 ng/ml; Invitrogen), epidermal growth factor (EGF, 10 ng/ml; Invitrogen), mouse platelet-derived growth factor bb (PDGFbb; 10 ng/ml; Invitrogen). Cells were seeded onto 25-cm^2 T-flask and incubated at 37 °C in 5 % CO_2 atmosphere. During the first week NSCs began to form neurospheres in vitro. At 2-day intervals, the neurospheres were collected and passaged by a gently enzymatic and mechanical dissociation. These processed NSCs retained the potential to proliferate indefinitely, as also demonstrated by their immunoreactivity for nestin, a marker for immature neural progenitors, which remained stable throughout the course of cell culture.

To obtain monolayer cultures, neurospheres of established cultures were passaged by enzymatic and mechanical dissociation and plated as single cells onto Matrigel Matrix (Becton Dickinson, Franklin Lakes, NJ) pre-coated Petri dishes. NSCs cultured in the medium described above, thereinafter referred to as "proliferation medium", remained in an undifferentiated state and proliferated. To induce differentiation, NSCs were cultured for up to 10 days in a medium defined as "differentiation medium", in which the FGF-2, EGF, and PDGFbb had been replaced with 1 % fetal calf serum.

In Vitro Proliferation Analysis of NSCs

BrdU incorporation was used to assess cell proliferation. Undifferentiated NSCs obtained by neurosphere dissociation were plated onto round coverslips and left to proliferate for 24 h. After this time period, BrdU (2.5 μM) was applied to the NSC culture medium and the cultures were either exposed to ELFEFs or left in control conditions for 6 and 24 h prior fixation (Fig. 1b). Dividing cells incorporating BrdU were identified by immunocytochemistry.

Immunocytochemistry

NSCs were processed for immunocytochemistry, as previously described [51, 52]. Briefly, cells were fixed with 4 % paraformaldehyde in PBS for 10 min at RT; rinsed twice in PBS; and permeabilized with PBS/TritonX-100 (0.3 %) for 15 min. For BrdU detection assays only, permeabilization was followed by 30 min incubation in 2 N HCl for DNA denaturation. Cells were then blocked with 0.3 % BSA in PBS and incubated overnight (at 4 °C) with one of the following antibodies (diluted in PBS): mouse anti-nestin for undifferentiated cells (1:500, Chemicon International, Inc., Temecula, CA, USA); mouse anti-MAP2 (1:300, clone HM-2; Sigma) for neurons; mouse anti-BrdU (1:300, clone BMC9318, Chemicon); and rabbit anti-phospho-cAMP response element-binding protein at Ser^{133} (anti-$pCREB^{Ser133}$, 1:400, Cell Signaling Technology, Danvers, MA, USA). The following day, cells were washed and incubated for 2 h at RT with secondary antibodies diluted in PBS: rhodamine-conjugated goat anti-mouse (1:300; Chemicon); and donkey anti-rabbit Alexa Fluor 488 (1:1,000, Molecular Probes). Nuclei were counterstained for 10 min with DAPI (0.5 mg/ml; Invitrogen) and finally cover-slipped with ProLong Gold antifade reagent (Molecular Probes).

Images (8 bits depth) were obtained with a confocal laser scanning system (TCS-SP2, Leica Microsystems) as described above. Double-blind counts of immunoreactive cells were performed in at least 10 random ×40 magnification fields for each experiment, and data were expressed as percentages of the total number of cells within the same fields (reflected by DAPI-counterstained nuclei). Experiments quantifying pCREB were analyzed by counting the number of cells exhibiting values of nuclear pCREB intensity higher than 150 over a range of 255 levels. All experiments were repeated independently at least three times.

Reverse Transcription-Quantitative PCR Analysis

All reverse transcription-quantitative PCR (RT-qPCR) experiments were performed as previously described [16, 53] with minor modifications. Sham- and ELFEF-exposed NSCs were examined for the expression of the bHLH transcription factors Hes1, Mash1, Neurogenin1 (Ngn1), and NeuroD1. Briefly, RNA was extracted from the cell pellets (RNeasy Micro, Ambion Inc., Austin, TX, USA) and residual DNA was removed (Turbo DNA-free kit, Ambion). Three experimental replicates were performed and RNA integrity and concentration were evaluated with the BioPhotometer plus (Eppendorf, Hamburg, Germany). Reverse transcription reactions were performed on equal amounts of RNA (2 μg) with a high-capacity cDNA reverse transcription kit (Applied Biosystems, Foster City, CA, USA). All RT-qPCR reactions were performed with inventoried TaqMan Gene expression assays purchased from Applied Biosystems. For each primer set, standard curves were plotted with several 10-fold dilutions of cDNA to ensure that the amplification was reliable and exponential. No-reverse-transcriptase control reaction was included in each experiment to ensure that all genomic DNA had been effectively removed. If any signal was detected in

this control reaction, the cDNA samples were discarded. Expression levels for genes of interest were normalized to levels measured for TATA-box-binding protein (TBP) and glyceraldehyde 3-phosphate dehydrogenase. Each experimental replicate was assessed in triplicate with the ABI 7500 Sequence Detection System analyzer for RT-qPCR (Applied Biosystems). The threshold cycle number furnished by the analyzer was normalized to the housekeeper and then used to calculate fold changes in gene expression with the $2^{-\Delta\Delta C}$ method [54]. Variations in gene expression induced by ELFEF exposure (vs. expression observed in unexposed control NSCs) were expressed as logged fold changes. For Neurogenin1 and NeuroD1 genes, that were not expressed in undifferentiated NSCs (time zero), variations in their expression were referred to the first time point at which their thresholds were measurable, and this value was taken as 1.0.

Chromatin Immunoprecipitation

Chromatin immunoprecipitation (ChIP) assays were performed as previously described [55]. For NSCs, ~1 to 3× 10^6 cells grown in proliferation and differentiation medium were used per ChIP (Fig. 1b). Briefly, at the end of stimulations, formaldehyde (1 %) was added directly to the medium for 10 min; afterward, medium was removed from treated cells and replaced with PBS containing protease inhibitors.

Six coronal brain sections containing hippocampi (Fig. 1a) were used for each animal (n=3 ELFEF-stimulated mice; n=3 sham-exposed mice). Hippocampal areas were isolated under optic microscope and minced through a 10 ml syringe with decreasing needle size (18 to 22 gauges).

Cell or tissue lysates were resuspended in 200 μl lysis buffer containing SDS (1 %), Tris–HCl (50 mM, pH 8.1), and EDTA (10 mM) and sonicated on ice with six 10-s pulses with a 20-s interpulse interval. Sample debris was removed by centrifugation, and supernatants were precleared by incubation with protein-G Sepharose 4B beads (Sigma) for 1 h at 4 °C. Beads were collected by centrifugation and supernatants were subjected to immunoprecipitation. A fraction of the supernatant was used for total input control. The volume of each tube was adjusted to 2 ml with dilution buffer (1 % Triton X-100, 1.2 mM EDTA, 16.7 mM Tris HCl at pH 8.1, 167 mM NaCl) and split in equal volumes for each immunoprecipitation (final SDS concentration 0.1 %). Two micrograms of specific antibody (anti-pCREB^{Ser133}, anti-acetyl histone H3K9 and anti-acetyl histone H4 from Millipore, anti-CBP and anti-HDAC2 from Abcam, anti-SIRT1 from Santa Cruz) or rabbit IgG were added overnight at 4 °C. Immune complexes were collected by incubation with protein-G Sepharose 4B beads for 2 h at 4 °C. Beads were collected and subjected to a series of seven sequential washes. Immune complexes were eluted from beads by vortexing in elution buffer containing SDS (1 %) and $NaHCO_3$ (0.1 M, pH 8.0). NaCl was added (final concentration 0.33 M), and cross-linking was reversed by incubation overnight at 65 °C. DNA fragments were purified by using the PCR DNA fragments purification kit (Geneaid). For PCR, specific sets of primers were designed that flank cAMP Responsive Elements (CRE) regions within the upstream regulatory regions of the indicated genes. PCR conditions and cycle numbers were determined empirically for the different templates and primer pairs. PCR for ChIP experiments were performed with the following pairs of primers:

Hes1 Forward AAGTAGTTATATTGCATGCAGC
Hes1 Reverse AGATCCTGTGTGATCCGCAG
NeuroD1 Forward CTGCTCGTTGCTCAGCTCACG
NeuroD1 Reverse CAAATATAGGGACAACCGACTCC
Ngn1 Forward GTGCCCAGGACGAAGAGCAGG
Ngn1 Reverse CCAGATGTAGTTGTAGGCGAAGC

In vitro experiments were repeated at least three times. Each PCR reaction was performed in triplicate (for a total of n=9 values per each condition). The results of densitometric analyses are indicated in the text. Values are expressed as means±SEM of fold changes (calculating the ratio between amplicon obtained from specific immunoprecipitation and that achieved from total chromatin input) compared with the relative control sample. In vivo experiments are shown by histograms displaying fold changes of the DNA fragments amplification (calculating by densitometric analysis the ratio between amplicon obtained from H3K9 acetylation or pCREB immunocomplexes and that achieved from total chromatin input) compared with the control group; values are means±SEM of n=3 mice. PCR analyses were repeated three times (for a total of n=9 values per each condition).

Western Blotting

For histone expression/acetylation studies cells were lysed in ice-cold lysis buffer (NaCl 150 mM, Tris–HCl 50 mM pH 8; 2 mM EDTA) containing 1 % Triton X-100, 0.1 % SDS, ×1 protease inhibitor mixture (Sigma), 1 mM sodium orthovanadate, and 1 mM NaF. After 15 min on ice with occasional vortexing, cells were spun down at 22,000×g, 4 °C to remove debris, and supernatant quantified for protein content (DC Protein Assay; Bio-Rad), resuspended in 6× Laemmli buffer, boiled, and resolved by SDS-PAGE. Anti-Ac-H3K9 rabbit anti-serum was from Millipore. Anti-Histone H3 mouse monoclonal antibody was from Abcam. Anti-tubulin mouse monoclonal antibody was from Sigma.

Statistical Analysis

Data are expressed as means±SEM. Statistical significance was assessed with ANOVA and Student's t test. For

experiments that included fewer than eight observations, the Mann–Whitney *U* test was used. The level of significance was set at 0.05.

Results

ELFEF-Stimulated Mice Show Improved Spatial Learning and Memory

We previously demonstrated that proliferation and neuronal differentiation of NSCs residing in the SGZ of the DG are markedly increased in C57bl/6 mice exposed to ELFEFs. The newborn neurons functionally integrated in the preexisting circuitry thus enhancing hippocampal synaptic plasticity [16]. To determine whether this ELFEF-induced increase in hippocampal neurogenesis is associated with improvement of spatial learning and hippocampal-dependent memory, we tested control and ELFEF-exposed mice with MWM and novel object recognition (NOR) paradigms. Both animal groups were subjected to behavioral tests about one month after completion of BrdU injection/ELFEF stimulation protocol (12D×3.5 h; Fig. 1a). This time period was needed to allow the functional integration of newborn neurons in the preexisting circuitry. At the end of behavioral tests mice were sacrificed to verify the ELFEFs' effect on hippocampal neurogenesis by immunohistochemical analysis. Compared with control (i.e., sham-exposed) animals, mice exposed to ELFEFs showed a significant reduction in the latency to find the hidden platform in all days of the training trials ($p<0.01$ vs. control on the 1st day; $p<0.05$ on the 2nd day; $p<0.001$ on the 3rd day; $p<0.01$ on the 4th day; Fig. 2a). Moreover, during the probe test performed 24 h after learning, the ELFEF-exposed mice displayed a significant increase in the time spent in the target quadrant (27.6±3.3 s), compared with control animals (19.5±1.8 s; two-way ANOVA; $F_{(3,122)}=21.4$; $p<0.05$; Fig. 2b).

We also used the NOR test to evaluate the ability of mice to discriminate novelty in a simple setting of two different objects. Consistently with the results described above, the ELFEF-exposed mice showed a higher discrimination ability compared with controls (preference index, 71.8 and 63.8 %, respectively; $p<0.001$; Fig. 2c).

Immunohistochemical analysis showed that improved memory correlated with enhanced neurogenesis. In particular, in mice exposed to ELFEFs the number of cells double labeled for the proliferation marker BrdU and the marker of immature neurons DCX ($BrdU^+/DCX^+$ cells) was significantly higher than in controls (11,160±805 vs. 6,993±1,433; $n=4$ mice for each group; $p<0.001$; Supplemental Fig. 1) 24 h after the completion of the ELFEF stimulation protocol. This difference was even larger when we counted the number of new cells that had become mature neurons ($BrdU^+/NeuN^+$ cells) 40 days after the exposure to ELFEFs (4,222±131 vs. 1,560±50 in controls; $p<0.005$; Supplemental Fig. 2).

Effects of ELFEF Stimulation on Hippocampal NSC Proliferation and Neuronal Differentiation

To identify the molecular mechanisms underlying the effects of ELFEFs on endogenous neurogenesis, we isolated and cultured hippocampal NSCs from newborn mice. We first analyzed the effects of ELFEF stimulation on the proliferation of undifferentiated NSCs (D0; Fig. 1b). The percentage of control NSCs incorporating BrdU was 37.2±3.7 % after 6 h of BrdU application and 70.9±3.3 % after 24 h. ELFEF stimulation significantly increased these rates to 56.3±1.9 and 77.1±2.5 %, respectively ($p<0.001$; Fig. 3a–c). Next, we studied the effects of continuous ELFEF exposure on neuronal differentiation of NSCs. To estimate the neuronal yields of NSC differentiation, we evaluated the immunoreactivity for the neuronal marker MAP2 in NSCs cultured for 6–10 days in the differentiation medium (D6 and D10, Fig. 1b). As shown in Fig. 3d, e, h, the neuronal differentiation of NSCs was enhanced by ELFEFs that increased the percentage of $MAP2^+$ cells from 23.5±1.5 % to 37.4±4.2 % ($p<0.001$) at D6, and from 32.4±3.9 to 45.5±4.1 % at D10 ($p<0.05$). In keeping with our previous findings obtained in a different in vitro model of NSCs [20, 52], treatment of ELFEF-exposed NSCs with the Ca_v1 channel blocker nifedipine (5 μM) significantly lowered the percentage of $MAP2^+$ cells to 15.6±1.6 % of total cells at D6 and to 24.6±3.0 % at D10 ($p<0.001$, Fig. 3g, h). Similarly, nifedipine inhibited neuronal differentiation in the sham-exposed NSCs (14.6±2.2 % $MAP2^+$ cells at D6 ($p<0.01$) and 21.5±1.0 % at D10 ($p<0.05$); Fig. 3f, h) thus confirming that Ca^{2+} signals produced via Ca_v1 channel activation have a pivotal role in controlling proliferation and neuronal differentiation of NSCs.

Effects of ELFEF Stimulation on Pro-Proliferative and Neuronal Differentiation Genes

To gain further insight on the molecular mechanisms subtending ELFEFs' effects on NSCs, we studied the temporal mRNA expression patterns of bHLH transcription factors including Hes1 (a component of the Notch signaling pathway involved in the modulation of cell proliferation and fate) and Mash1, Neurogenin1 and NeuroD1 (which play critical roles in fate determination and neuronal differentiation) [25–28]. Real-time RT-qPCR analysis revealed that the ELFEF-induced proliferation of hippocampal NSCs is associated with the upregulation of the pro-proliferative gene Hes1 expression at D0 (Fig. 4a). Subsequently, during 6–12 h differentiation we observed a more marked downregulation of Hes1 expression in ELFEF-exposed cells followed by a rebound effect observed at 24 h. Downregulation of Hes1 expression was

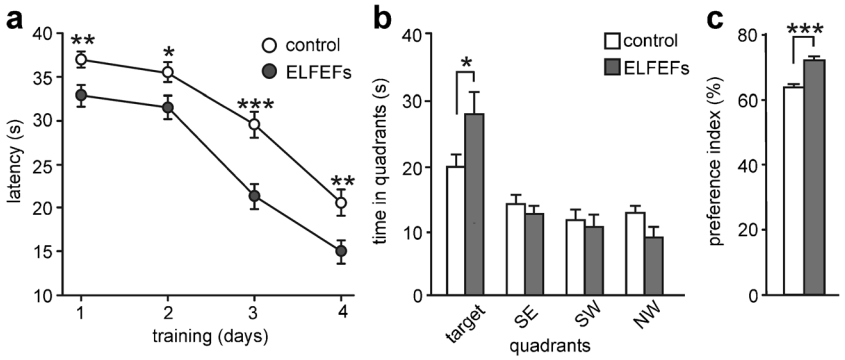


Fig. 2 Effect of ELFEF exposure on mouse memory performance in the MWM and NOR tests. **a** Escape latency to reach the hidden platform of control and ELFEF-exposed mice and **b** time spent in the four quadrants during probe test performed on day 5 of MWM test. ELFEF-exposed mice showed reduced latencies to find escape platform and spent more time in the target quadrant during the probe test compared with controls. **c** Preference toward the novel object in NOR paradigm. ELFEF-exposed mice spent more time exploring the novel object and less time exploring the familiar object compared with control animals. Values are mean± SEM (n=14 for control and n=16 for ELFEF-exposed mice in MWM test; n=8 for each group in NOR test. *p<0.05; **p<0.01; ***p<0.001)

accompanied by an upregulation of the neuronal determination gene, Mash1, and of the differentiation genes, Neurogenin1 and NeuroD1 (Fig. 4a–d). Moreover NSC exposure to ELFEFs accelerated Mash1 expression, thus anticipating its upregulation and the consequent neuronal commitment of NSCs. In particular, the peak Mash1 expression occurred at 12 h differentiation in control NSCs and at 6 h in the ELFEF-exposed cultures (Fig. 4b).

Given that the different bHLH transcription factors are reportedly modulated by changes in intracellular Ca^{2+}

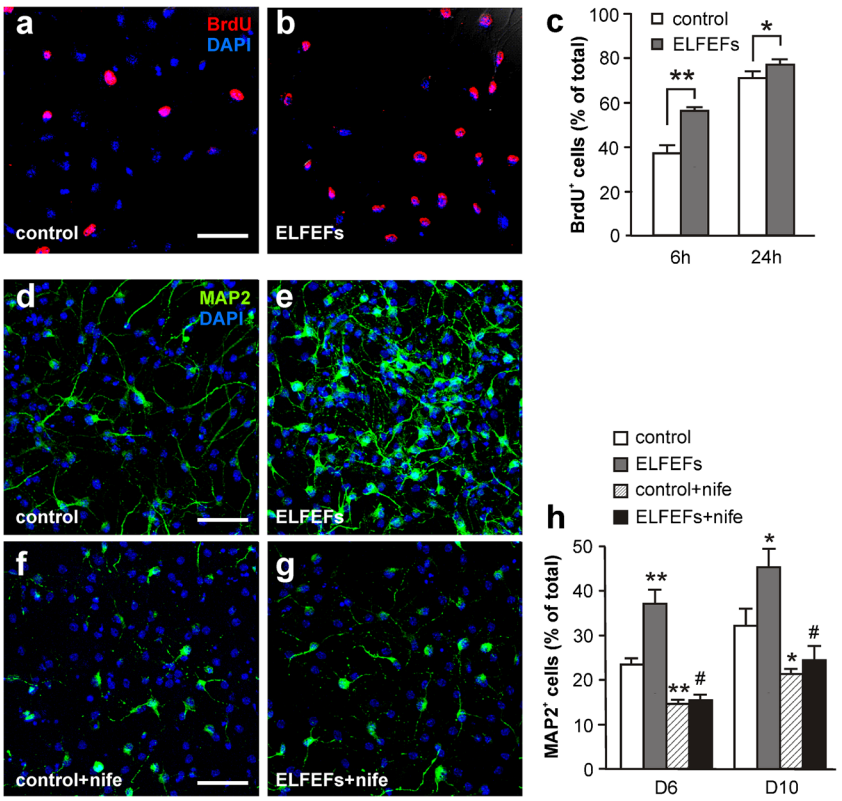


Fig. 3 Effect of ELFEF exposure on proliferation and differentiation of hippocampal NSCs. Representative images of BrdU incorporation in control NSC cultures (**a**) and cultures exposed to ELFEFs (**b**) 6 h after addition of 2.5 μM BrdU to the proliferation medium. **c** *Bar graph* showing the percentages of NSCs incorporating BrdU after 6 and 24 h exposures to ELFEFs compared with control NSCs. **d**, **e** Representative images of differentiating NSCs at D6 immunoreactive to the neuronal marker, MAP2, in control conditions (**d**) and after exposure to ELFEFs (**e**). **f**, **g** The Ca_V1-channel blocker nifedipine-reduced (5 μM) MAP2 positivity rates in both unexposed (**f**) and ELFEF-exposed (**g**) cells at D6. **h** *Bar graph* showing the percentages of $MAP2^+$ cells at D6 and D10 under control and ELFEF exposure condition in the presence and absence of nifedipine. *p<0.05; **p<0.001 vs. controls; #p<0.001 vs. ELFEFs. *Scale bar*, 75 μm

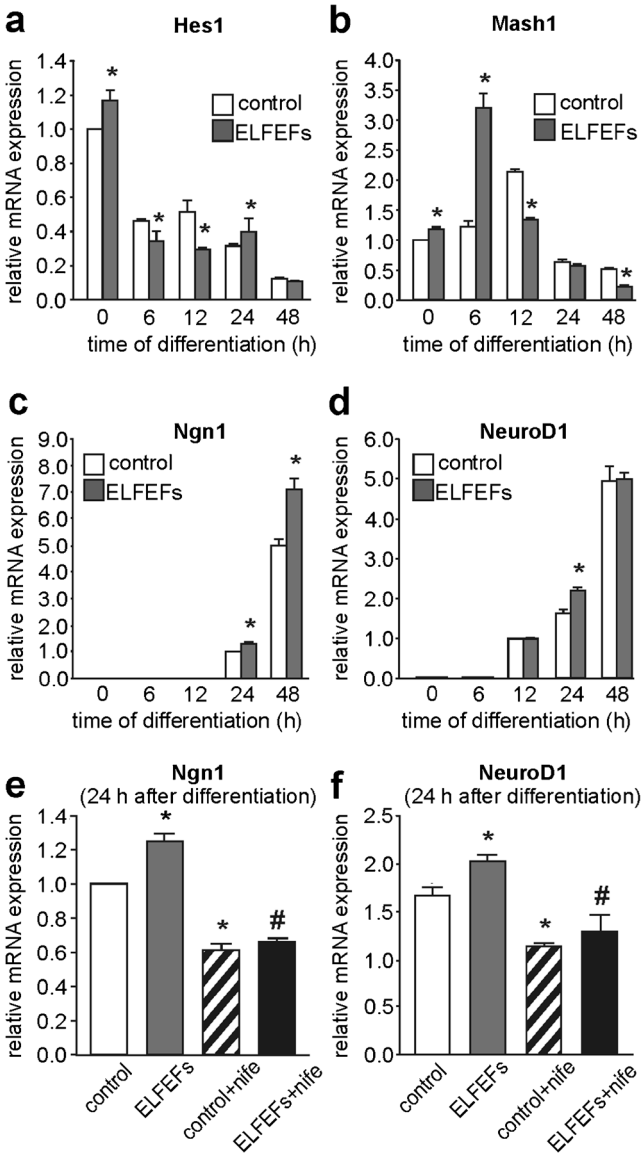


Fig. 4 ELFEF stimulation modulates NSC expression of pro-neuronal transcription factors. **a** Levels of mRNA encoding for Hes1 were increased in undifferentiated (time point, 0) NSCs grown for 24 h in presence of ELFEF stimulation. During NSC differentiation (from 6 to 48 h) mRNA levels of Mash1 (**b**), Neurogenin1 (*Ngn1*; **c**), and NeuroD1 (**d**) were significantly increased by ELFEF exposure, whereas Hes1 expression was decreased. Twenty-four hours of NSC differentiation in the presence of the Ca_v1-channel blocker nifedipine (5 μM) inhibited the expression of both Ngn1 (**e**) and NeuroD1 (**f**) mRNAs and prevented their increase in response to ELFEF exposure. Values are expressed as means± SEM of the fold increase in the ratio of each gene/TBP, with the value of control undifferentiated NSCs (time point, 0) taken as 1.0. In (**c**)–(**f**), as both Ngn1 and NeuroD1 were not expressed and detectable in undifferentiated NSCs (time zero), their relative mRNA levels are expressed as means±SEM of the fold increase, with the value of control differentiating NSCs at the first time point detectable taken as 1.0. *$p<0.05$ vs. control unexposed NSCs. #$p<0.05$ vs. ELFEFs

concentration [56–59], we asked whether this mechanism could account for the observed Ca_v1 channel-dependent effects of ELFEFs on NSC neuronal differentiation. We therefore studied the effects of ELFEFs on both Neurogenin1 and NeuroD1 levels in the presence of nifedipine (5 μM). In agreement with our immunofluorescence data, the blockade of Ca_v1 channels significantly lowered the expression of Neurogenin1 and NeuroD1 mRNAs (−38.6 and −31 %; $p<0.05$) and prevented their increases we observed after 24 h of exposure to ELFEFs (+24 and +35 %, respectively) in nifedipine-free cultures (Fig. 4e, f; $p<0.01$).

ELFEF Stimulation Induces Trans-regulatory Factor Modifications on Neuronal Differentiation Gene Promoters: Acetylation of Histone H3 on Lysine 9 and Binding of Transcription Factor CREB and Histone Acetyltransferase CBP

To investigate if Ca_v1 channel mediated effects of ELFEFs on bHLH gene expression could involve the regulation of the transcriptional machinery assembly, we analyzed the calcium-dependent modulation of CREB phosphorylation upon ELFEF stimulation and evaluated its binding to regulatory sequences on the bHLH genes. Immunofluorescence experiments indicated that the percentage of differentiating cells exhibiting high levels of $pCREB^{Ser133}$ (see "Materials and Methods") was significantly increased (+180 %) by 24-h exposure to ELFEFs (from D0 to D1) and this effect was prevented by the presence of 5 μM nifedipine in the culture medium. In particular, cells exhibiting increased level of pCREB accounted for 13.4±1.9 % of all cells in control cultures (Fig. 5a, e) and rose to 37.6±5.6 % in ELFEF-exposed cultures (Fig. 5b, e). Nifedipine markedly reduced the percentage of $pCREB^{+}$ cells in control and ELFEF-exposed cultures to 1.3±1.6 and 2.6±1.1 %, respectively (Fig. 5c–e).

Data presented so far suggest that the ELFEF-mediated neuronal differentiation of NSCs is preceded by the phosphorylation of CREB and the subsequent expression of pro-neuronal genes. These genes may represent direct transcriptional targets of CREB. Bioinformatic analysis of the mouse NeuroD1 and Neurogenin1 loci revealed the presence of a putative CRE region on the regulatory sequence of both genes, located downstream the transcription start site (+58 for NeuroD1 and +285 for Neurogenin1). We tested whether exposure of NSCs to ELFEFs mediates changes in histone acetylation (as marker of gene transcription activation) and in CREB binding to neuronal gene promoters. We used the ChIP assays with anti-acetyl histone H3K9, anti-acetyl histone H4 and anti-phospho-CREB antibodies. CREB was found to interact with both genes, in a fashion inducible by ELFEFs (+19.8±1.2 % for Neurogenin1 and +50.4±2.3 % for NeuroD1; $p<0.05$) and with a binding kinetic similar to that of H3K9 acetylation (+24.7±1.3 and +40.1±2.3 % respectively; $p<0.05$) (Fig. 6a, b). Conversely, pan acetylation of histone H4 on the NeuroD1 and Neurogenin1 analyzed

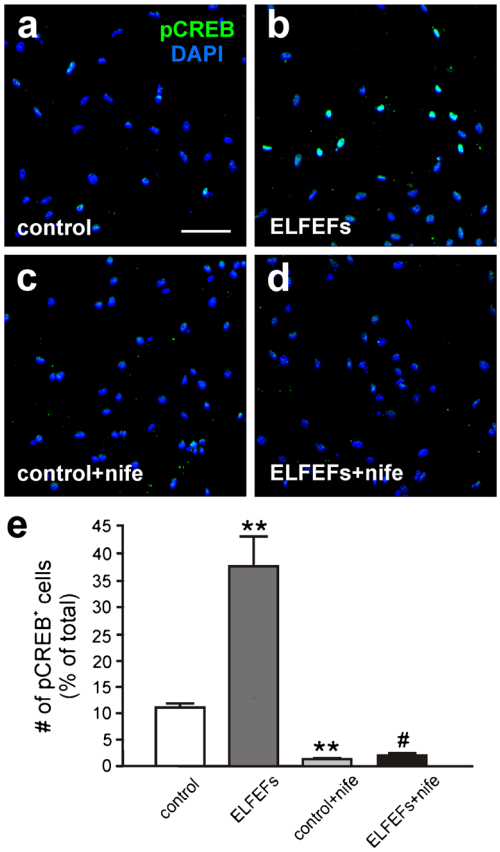


Fig. 5 Effect of ELFEFs on CREB phosphorylation. Representative images of pCREB immunoreactivity in control NSCs at D1 (**a**), in NSCs exposed to ELFEFs (**b**), and in control and exposed NSCs in the presence of the selective Ca_v1 channel inhibitor nifedipine (5 μM) (**c**, **d**, respectively). **e** *Bar graph* quantifying the percentages of differentiating NSCs at D1 expressing high levels of $pCREB^{Ser133}$ in the conditions listed above. Cell nuclei were stained with DAPI. $^{**}p<0.001$ vs. control; # $p<0.001$ vs. ELFEFs. *Scale bar*, 75 μm

sequences was not modified by ELFEF stimulation (data not shown). Interestingly, these epigenetic effects were prevented by nifedipine, thus confirming a pivotal role of Ca_v1 channel signaling for the neuro-differentiating program activated by ELFEFs.

Given the enhanced proliferation of NSCs, we observed following ELFEF stimulation and evaluated the H3K9 acetylation on Hes1 promoter region. Our results showed that ELFEFs increased the level of H3K9 acetylation on this promoter (+71.8±3.3 %; $p<0.05$) in undifferentiated NSCs, and this effect was inhibited by nifedipine (Fig. 6c). Expectedly, Hes1 promoter acetylation was not present in NSCs that had been grown for 24 h in differentiation medium in both control and ELFEF-exposed cells. Consistent with the role of CREB as a histone acetyltransferase/deacetylase recruiter we also investigated the binding of other regulatory proteins to bHLH gene promoters upon ELFEF stimulation. CBP is a histone acetyltransferase that cooperates to gene transcription activation, whereas HDAC2 and SIRT1 are histone deacetylases involved in gene silencing. We performed additional ChIP assays to determine their recruitment to the bHLH regulatory sequences. DNA analysis showed an ELFEF-dependent increase of CBP binding to Neurogenin1 and NeuroD1 promoters (+32.7±2.1 and +53.2±4.3 % respectively; $p<0.05$) in differentiating NSCs (Fig. 6d, e) and to Hes1 (+35.3±2.6 %; $p<0.05$) under proliferative condition (Fig. 6f). The recruitment of SIRT1 was slightly but not significantly modified on these loci upon ELFEF stimulation. In particular, SIRT1 binding to NeuroD1 and Hes1 promoters decreased in proliferative and differentiative condition, respectively, in line with the increase of H3 acetylation upon ELFEF stimulation (Fig. 6e, f). To check whether histone H3 acetylation was increased globally in genome-wide manner rather than specifically at the pro-neuronal gene promoters in response to ELFEF stimulation, we performed a Western blotting analysis on NSC lysates. Results revealed no significant changes of H3K9 acetylation on NSCs exposed to ELFEFs (Supplemental Fig. 3).

Overall, these data indicate that the ELFEF regulation of NSC gene expression is associated with several epigenetic events: the CBP recruitment, the Ca_v1-dependent binding of pCREB and histone H3K9 acetylation on the regulatory sequence of pro-proliferative and neuronal determination genes.

In Vivo Exposure to ELFEFs Confirms Epigenetic Modifications Observed on Neuronal Differentiation Gene Promoters in Vitro

We next asked whether ELFEFs also regulate histone acetylation and pCREB binding to the Neurogenin1 and NeuroD1 promoters in vivo. Six hippocampal sections obtained from each ELFEF- or sham-exposed mouse ($n=3$ for each group), obtained as described in "Materials and Methods," were analyzed by chromatin immunoprecipitation. Our results showed that also in vivo ELFEF stimulation elicited the recruitment of CREB activated form on neuronal differentiation gene promoters, concomitantly with acetylation of H3K9 on these regulatory regions (Fig. 7a, b).

Discussion

In the present study, we show that in vitro exposure of hippocampal NSCs to ELFEFs enhances their proliferation and neuronal cell-fate specification by a Ca_v1-channel-dependent regulation of H3K9 acetylation and pCREB levels at specific bHLH neuronal gene promoters. Histone acetyltransferase CBP is also involved in the epigenetic events underlying ELFEF-induced regulation of gene expression. Moreover, experiments performed in vivo on adult mice exposed to ELFEFs demonstrate that enhanced hippocampal neurogenesis and epigenetic modifications similar to those observed in vitro are associated with spatial learning and

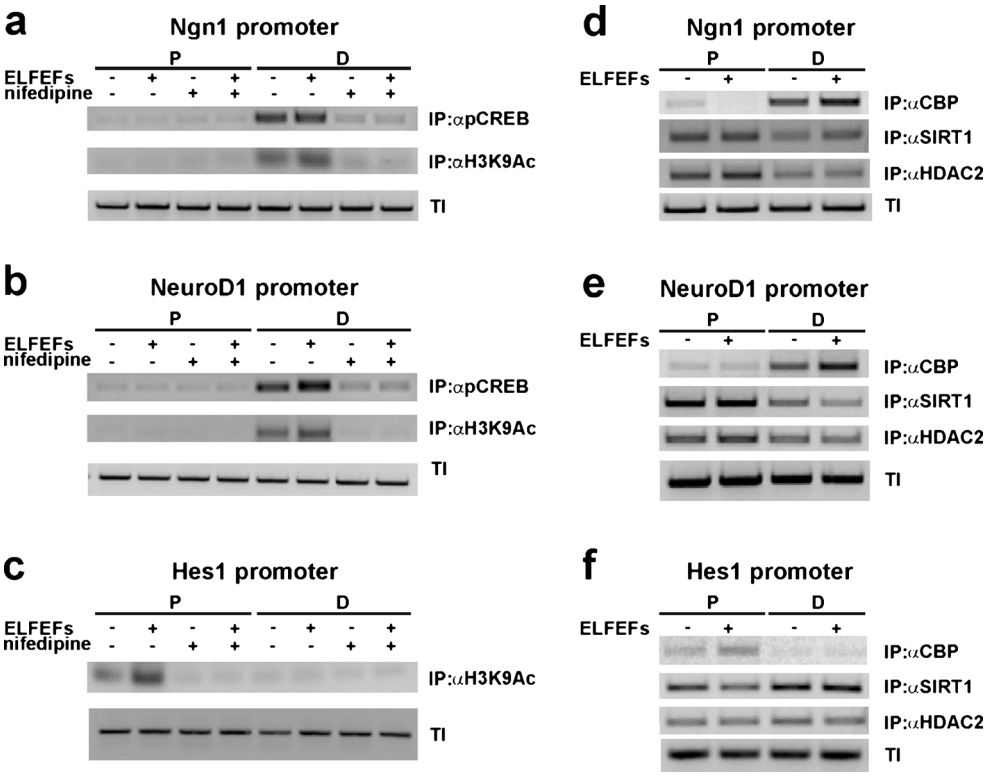


Fig. 6 ELFEFs' effects on bHLH neuronal gene promoters of hippocampal NSCs. ChIP assays were performed on control and ELFEF-exposed NSCs in both proliferative (*P*) and differentiative (*D*) culture conditions, with or without nifedipine (5 μM). Neurogenin1 (*Ngn1*; **a**), NeuroD1 (**b**), and Hes1 (**c**) promoter fragments were amplified from the pCREB and acetyl H3K9 immunoprecipitated DNA or from the total chromatin input as quantitative control (*TI*). CBP, SIRT1 and HDAC2 recruitment on the same regulatory sequences is visualized by chromatin analyses of Ngn1 (**d**), NeuroD1 (**e**) and Hes1 (**f**) promoters. The results of densitometric analyses are indicated in the text

memory improvements. These findings take on particular relevance given the crucial role of newborn neurons in learning and memory [4, 6] and the great potential of enhancing hippocampal neurogenesis for treatment of cognitive disorders.

We found that at the end of the stimulation protocol (12D× 3.5 h) the number of immature newborn neurons (revealed as $BrdU^+/DCX^+$ cells within the granular cell layer of the DG) was 60 % higher in ELFEF-exposed mice than in controls. Moreover, one month after completion of the BrdU injection/

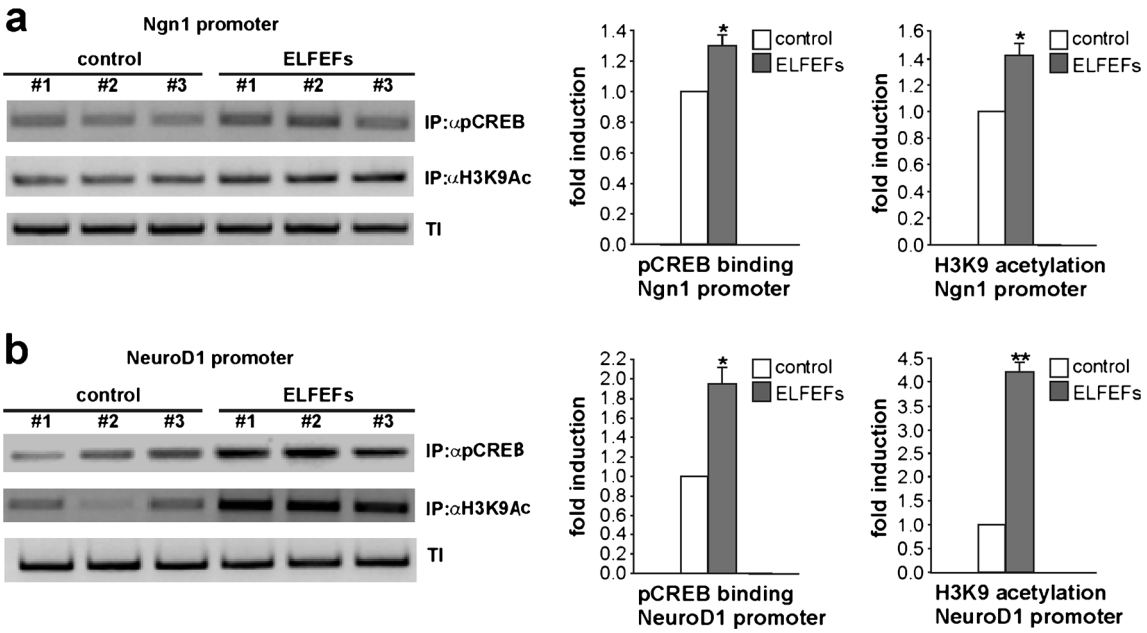


Fig. 7 ELFEFs' effects on bHLH neuronal gene promoters of mouse hippocampi. ChIP assays performed on hippocampal extracts of control (n=3) and ELFEF-exposed mice (n=3). Neurogenin1 (*Ngn1*; **a**) and NeuroD1 (**b**) promoter fragments were amplified from the pCREB and acetyl H3K9-immunoprecipitated DNA or from the total chromatin input as quantitative control (*TI*). Each experiment was repeated three times. On the right, bar graph showing mean±SEM values of normalized data expressed as fold increase in the ratio of each gene/TI, with the value of control hippocampi taken as 1.0. *p<0.05; **p<0.01

ELFEF stimulation protocol, mice exposed to ELFEFs displayed an increased number (+171 %) of BrdU/NeuN double-positive cells compared with control animals, thus suggesting that ELFEFs also enhance survival and maturation of new neurons in the DG. Data from immunohistochemistry are fully consistent with our birthdating experiments in which we used a different ELFEF stimulation protocol (i.e., 7D×7 h). The protocol used in this study (12D×3.5 h) appeared to us, in a future perspective, more suitable for the use of ELFEF stimulation in clinical settings.

In this respect, it is worth noting that nowadays several studies have explored the biological effects of ELFEFs (0–300 Hz) on the nervous system in the intact human brain and reported several functional changes [60, 61].

Our present study points to ELFEF stimulation as a good tool to enhance hippocampal neurogenesis and improve hippocampal-dependent memory functions in mice. The optimization of stimulation protocol and the characterization of ELFEF's mechanisms at molecular levels in the animal model appear pivotal for translating results to humans. Within this horizon, we extended our study on ELFEFs' effects to an in vitro model of hippocampal NSCs. BrdU incorporation experiments revealed that exposure of undifferentiated NSCs to ELFEFs significantly increases their proliferation and this effect is associated with enhanced upregulation of Hes1 mRNA level. A large body of evidence demonstrated that Hes1 is a repressor type of bHLH transcriptional factor that regulates the maintenance of NSCs by repressing pro-neural gene expression [24]. Conversely, inactivation of Hes1 upregulates the expression of pro-neural genes (as Mash1, Neurogenin1, and NeuroD1) thus accelerating neuronal differentiation [62–64]. In particular, Mash1 defines cells with long-term neurogenic potential in the SGZ and subventricular zones of adult mouse brain [26], whereas NeuroD1 induces terminal neuronal differentiation during neurogenesis [25]. Our in vitro findings are consistent with this Hes1-dependent switch between promotion of NSC proliferation and activation of their neuronal differentiation. In fact, exposure of differentiating NSCs to ELFEFs enhances their neuronal differentiation by increasing the upregulation of Mash1, Neurogenin1, and NeuroD1 mRNAs and, at once, by enhancing the downregulation of Hes1. These events precede the increased percentages of cells acquiring the neuronal marker MAP2 in ELFEF-exposed cultures, as revealed by immunocytochemical analysis. The rebound effect we observed in Hes1 expression at 24 h after differentiation in ELFEF-exposed NSCs is in line with the oscillatory Hes1 expression pattern described in previous studies [65, 66]. In particular, it has been shown that Hes1 represses its own expression by directly binding to its promoter and this negative feedback leads to the disappearance of Hes1 mRNA and protein allowing the next round of its expression. This oscillatory Hes1 expression leads neural stem/progenitor cells to proliferate actively and differentiate into mature cells.

With regard to the time course of Mash1, acceleration of its expression profile by ELFEFs resulted in a global increase in the neuronal yield of NSC differentiation as revealed by both in vitro and in vivo immunofluorescence analyses. These findings are in agreement with what has been observed in response to other neurogenic stimuli [67, 68].

In previous studies, we demonstrated that ELFEF stimulation of neuroendocrine cells and cortical NSCs upregulates the expression and activity of voltage-gated Ca^{2+} channels, and the increased intracellular Ca^{2+} signaling generated by Ca_v1 channel activation plays a pivotal role in a number of cellular functions including the neuronal differentiation of NSCs [20, 43, 52, 69]. The role played by Ca_v1 channels in ELFEF-induced differentiation was also documented in rat chromaffin cells in which ELFEFs markedly affected gene expression [70, 71]. We also demonstrated that, in vivo, ELFEF-enhanced adult hippocampal neurogenesis is associated with increased expression of both bHLH neuronal genes and Ca_v1 channels [16]. Ca^{2+} signaling is known to affect the transcription of numerous genes, including bHLH transcriptional factors and the activation of CREB [57, 72–74]. On the other hand, CREB, as a master switch of Ca^{2+}-triggered transcriptional programs, plays important roles in adult neurogenesis [75, 76] and cognition [55, 77]. Here, we provide evidence that exposure of differentiating NSCs to ELFEFs induces Ca_v1-dependent CREB phosphorylation, which is involved in the regulation of neuronal gene expression. In fact, the increased phosphorylation of CREB at Ser^{133} induced by ELFEFs in differentiating NSCs, together with NeuroD1 and Neurogenin1 transcriptional increments are prevented by the Ca_v1 channel blocker, nifedipine. These events are followed by a significant drop of ELFEF-induced increase in neuronal differentiation in the presence of nifedipine. Consistently, with our present results, Ramirez and coworkers [73] recently showed that the pharmacological blockade of CREB activity inhibited the Ca^{2+}-dependent NeuroD1 expression triggered by GABA receptor stimulation in retinal progenitor cells.

Increasing evidence suggests that chromatin modifications play a critical role in the regulation of progenitor cell differentiation and increased histone acetylation is associated with neuronal lineage progression [31, 33]. In agreement with such function of histone acetylation and the role of CREB as a recruiter of histone acetyltrasferases, we demonstrated that ELFEF exposure of differentiating NSCs increases histone H3K9 acetylation and pCREB binding to NeuroD1 and Neurogenin1 promoters. These events rely on Ca^{2+} signals through voltage-dependent Ca^{2+} channels since they were inhibited in presence of nifedipine and were concurrent with the Ca_v1-dependent effect of ELFEFs on NeuroD1 and Neurogenin1 mRNA expressions. Histone acetylation, such as H3K9, is regulated by histone deacetylases (HDACs) and

histone acetyltransferases, and is associated with open chromatin and increased transcription. CBP is a histone acetyltransferase that cooperates with CREB in a large number of molecular pathways [78] and regulates embryonic neural differentiation in the brain [79]. Its activity is counteracted by several transcription repressors including SIRT1 [80], a protein deacetylase belonging to the family of sirtuins, that regulates proliferation of neural progenitor cells [81], and HDAC2 [82], a HDAC involved in the commitment of NSCs to a neurogenic lineage in the hippocampus [83]. The recruitment of CBP on the regulatory sequence of bHLH gene was enhanced by ELFEF stimulation, whereas binding of the HDACs was not significantly modulated by ELFEFs. In accordance with our results, Chatterjee and coworkers [84] recently showed that a CBP activator promotes neurogenesis and long-term memory in adult mice. Increased acetylation of histone H3K9 and pCREB binding at NeuroD1 and Neurogenin1 promoters were also found on hippocampal extracts from ELFEF-exposed mice. These data suggest that chromatin remodeling at specific neuronal gene promoters underlies the ELFEFs' effects on adult hippocampal neurogenesis in vivo.

In several models histone acetylation promotes NSC differentiation [85, 86]. Our data support this idea and suggest that the transcription factor CREB plays an important role in regulating gene expression in developing neurons via the control of histone acetylation. Phosphorylated CREB recruitment and histone H3 acetylation on the key pro-neural differentiating genes appear to be dependent on Ca^{2+} signals. A possible mechanism may be that intracellular Ca^{2+} stimulates phosphorylation of transcription factor CREB and assembly of transcriptional machinery, including histone acetyltransferase. Alternatively, calcium or other ELFEF-activated signals could induce histone modifications and chromatin unravelling, leading to the CREB binding and the start of transcription. Consistently with our results a role for Ca_v1-channels in facilitating histone H3 acetylation was also described in the limbic forebrain [87].

Finally, with regard to the genes modulated by ELFEFs in differentiating NSCs, we provide novel evidence that Neurogenin1 and NeuroD1 are CREB target genes in the nervous system. There is some evidence about an indirect functional interaction between CREB activation and Neurogenin2 expression in the subventricular zone progenitor cells [88] and, more importantly, with NeuroD1 in insulin-producing β-cells [89]. Nevertheless, we provided the first evidence of the capacity of CREB to bind several sequences on the promoters of these genes in the NSCs. These findings have important implications, as it has been suggested that NeuroD1 loss of function is involved in the pathogenesis of brain disorders, like epilepsy [90] and Huntington's disease [91].

In conclusion, our study identifies a novel molecular mechanism responsible for ELFEF-induced enhancement of hippocampal neurogenesis, which is of potential relevance for future stem cell-based therapeutic approaches. The discovery of the new CREB/NeuroD1 axis may be also relevant for treatment of brain disorders associated to alterations of these transcription factors.

Acknowledgments This work was supported by grants from the Italian Ministry of Health (RF-2009-1543811) and from the Catholic University (D3.2 and D1 funds).

References

1. Kempermann G, Wiskott L, Gage FH (2004) Functional significance of adult neurogenesis. Curr Opin Neurobiol 14:186–191
2. Ming GL, Song H (2011) Adult neurogenesis in the mammalian brain: significant answers and significant questions. Neuron 70: 687–702
3. Zhao C, Teng EM, Summers RG Jr et al (2006) Distinct morphological stages of dentate granule neuron maturation in the adult mouse hippocampus. J Neurosci 26:3–11
4. Aimone JB, Deng W, Gage FH (2011) Resolving new memories: a critical look at the dentate gyrus, adult neurogenesis, and pattern separation. Neuron 70:589–596
5. Kee N, Teixeira CM, Wang AH et al (2007) Imaging activation of adult-generated granule cells in spatial memory. Nat Protoc 2:3033–3044
6. Marín-Burgin A, Schinder AF (2012) Requirement of adult-born neurons for hippocampus-dependent learning. Behav Brain Res 227:391–399
7. Shors TJ, Miesegaes G, Beylin AV et al (2001) Neurogenesis in the adult is involved in the formation of trace memories. Nature 410: 372–376
8. Vivar C, van Praag H (2013) Functional circuits of new neurons in the dentate gyrus. Front Neural Circuits 7:15
9. Bellenchi GC, Volpicelli F, Piscopo V et al (2013) Adult neural stem cells: an endogenous tool to repair brain injury? J Neurochem 124: 159–167
10. Encinas JM, Sierra A (2012) Neural stem cell deforestation as the main force driving the age-related decline in adult hippocampal neurogenesis. Behav Brain Res 227:433–439
11. Taylor CJ, Jhaveri DJ, Bartlett PF (2013) The therapeutic potential of endogenous hippocampal stem cells for the treatment of neurological disorders. Front Cell Neurosci 7:5
12. Brown J, Cooper-Kuhn CM, Kempermann G et al (2003) Enriched environment and physical activity stimulate hippocampal but not olfactory bulb neurogenesis. Eur J Neurosci 17:2042–2046
13. Kempermann G (2012) New neurons for 'survival of the fittest'. Nat Rev Neurosci 13:727–736
14. van Praag H, Christie BR, Sejnowski TJ et al (1999) Running enhances neurogenesis, learning, and long-term potentiation in mice. Proc Natl Acad Sci U S A 96:13427–13431
15. Arias-Carrión O, Verdugo-Díaz L, Feria-Velasco A et al (2004) Neurogenesis in the subventricular zone following transcranial magnetic field stimulation and nigrostriatal lesions. J Neurosci Res 78: 16–28
16. Cuccurazzu B, Leone L, Podda MV et al (2010) Exposure to extremely low-frequency (50 Hz) electromagnetic fields enhances adult hippocampal neurogenesis in C57BL/6 mice. Exp Neurol 226:173–182
17. Podda MV, Leone L, Barbati SA et al. (2014) Extremely low-frequency electromagnetic fields enhance the survival of newborn neurons in the mouse hippocampus. Eur J Neurosci

18. Czéh B, Welt T, Fischer AK et al (2002) Chronic psychosocial stress and concomitant repetitive transcranial magnetic stimulation: effects on stress hormone levels and adult hippocampal neurogenesis. Biol Psychiatry 52:1057–1065
19. Hansson Mild K, Alanko T, Decat G et al (2009) Exposure of workers to electromagnetic fields. A review of open questions on exposure assessment techniques. Int J Occup Saf Ergon 15:3–33
20. Piacentini R, Ripoli C, Mezzogori D et al (2008) Extremely low-frequency electromagnetic fields promote in vitro neurogenesis via upregulation of Ca(v)1-channel activity. J Cell Physiol 215:129–139
21. Hsieh J (2012) Orchestrating transcriptional control of adult neurogenesis. Genes Dev 26:1010–1021
22. Nieber F, Pieler T, Henningfeld KA (2009) Comparative expression analysis of the neurogenins in *Xenopus tropicalis* and *Xenopus laevis*. Dev Dyn 238:451–458
23. Sommer L, Ma Q, Anderson DJ (1996) Neurogenins, a novel family of atonal-related bHLH transcription factors, are putative mammalian neuronal determination genes that reveal progenitor cell heterogeneity in the developing CNS and PNS. Mol Cell Neurosci 8:221–241
24. Bai G, Sheng N, Xie Z et al (2007) Id sustains Hes1 expression to inhibit precocious neurogenesis by releasing negative autoregulation of Hes1. Dev Cell 13:283–297
25. Boutin C, Hardt O, de Chevigny A et al (2010) NeuroD1 induces terminal neuronal differentiation in olfactory neurogenesis. Proc Natl Acad Sci U S A 107:1201–1216
26. Kim EJ, Ables JL, Dickel LK et al (2011) Ascl1 (Mash1) defines cells with long-term neurogenic potential in subgranular and subventricular zones in adult mouse brain. PLoS ONE 6:e18472
27. Lo L, Tiveron MC, Anderson DJ (1998) MASH1 activates expression of the paired homeodomain transcription factor Phox2a, and couples pan-neuronal and subtype-specific components of autonomic neuronal identity. Development 125:609–620
28. Sun Y, Nadal-Vicens M, Misono S et al (2001) Neurogenin promotes neurogenesis and inhibits glial differentiation by independent mechanisms. Cell 104:365–376
29. Jenuwein T, Allis CD (2001) Translating the histone code. Science 293:1074–1080
30. Crepaldi L, Riccio A (2009) Chromatin learns to behave. Epigenetics 4:23–26
31. Gräff J, Tsai LH (2013) Histone acetylation: molecular mnemonics on the chromatin. Nat Rev Neurosci 14:97–111
32. Lee S, Lee SK (2010) Crucial roles of histone-modifying enzymes in mediating neural cell-type specification. Curr Opin Neurobiol 20:29–36
33. Olynik BM, Rastegar M (2012) The genetic and epigenetic journey of embryonic stem cells into mature neural cells. Front Genet 3:81
34. Cho B, Kim HJ, Kim H et al (2011) Changes in the histone acetylation patterns during the development of the nervous system. Exp Neurobiol 20:81–84
35. Lilja T, Heldring N, Hermanson O (2013) Like a rolling histone: epigenetic regulation of neural stem cells and brain development by factors controlling histone acetylation and methylation. Biochim Biophys Acta 1830:2354–2360
36. Day JJ, Sweatt JD (2011) Epigenetic mechanisms in cognition. Neuron 70:813–829
37. Miller CA, Campbell SL, Sweatt JD (2008) DNA methylation and histone acetylation work in concert to regulate memory formation and synaptic plasticity. Neurobiol Learn Mem 89:599–603
38. Roth TL, Sweatt JD (2009) Regulation of chromatin structure in memory formation. Curr Opin Neurobiol 19:336–342
39. Sharma SK (2010) Protein acetylation in synaptic plasticity and memory. Neurosci Biobehav Rev 34:1234–1240
40. Sui L, Wang Y, Ju LH et al (2012) Epigenetic regulation of reelin and brain-derived neurotrophic factor genes in long-term potentiation in rat medial prefrontal cortex. Neurobiol Learn Mem 97:425–440
41. Gräff J, Mansuy IM (2009) Epigenetic dysregulation in cognitive disorders. Eur J Neurosci 30:1–8
42. Tsankova N, Renthal W, Kumar A et al (2007) Epigenetic regulation in psychiatric disorders. Nat Rev Neurosci 8:355–367
43. Grassi C, D'Ascenzo M, Torsello A et al (2004) Effects of 50 Hz electromagnetic fields on voltage-gated Ca^{2+} channels and their role in modulation of neuroendocrine cell proliferation and death. Cell Calcium 35:307–315
44. Wolf FI, Torsello A, Tedesco B et al (2005) 50-Hz extremely low frequency electromagnetic fields enhance cell proliferation and DNA damage: possible involvement of a redox mechanism. Biochim Biophys Acta 1743:120–129
45. Kempermann G, Gage FH (2002) Genetic determinants of adult hippocampal neurogenesis correlate with acquisition, but not probe trial performance, in the water maze task. Eur J Neurosci 16:129–136
46. Leone L, De Stefano ME, Del Signore A et al (2005) Axotomy of sympathetic neurons activates the metalloproteinase-2 enzymatic pathway. J Neuropathol Exp Neurol 64:1007–1017
47. Podda MV, D'Ascenzo M, Leone L et al (2008) Functional role of cyclic nucleotide-gated channels in rat medial vestibular nucleus neurons. J Physiol 586:803–815
48. Podda MV, Leone L, Piacentini R et al (2012) Expression of olfactory-type cyclic nucleotide-gated channels in rat cortical astrocytes. Glia 60:1391–1405
49. Mayhew TM, Gundersen HJ (1996) If you assume, you can make an ass out of u and me': a decade of the disector for stereological counting of particles in 3D space. J Anat 188:1–15
50. West MJ (1999) Stereological methods for estimating the total number of neurons and synapses: issues of precision and bias. Trends Neurosci 22:51–61
51. Podda MV, Piacentini R, Barbati SA et al (2013) Role of cyclic nucleotide-gated channels in the modulation of mouse hippocampal neurogenesis. PLoS ONE. doi:10.1371/journal.pone.0073246
52. D'Ascenzo M, Piacentini R, Casalbore P et al (2006) Role of L-type Ca^{2+} channels in neural stem/progenitor cell differentiation. Eur J Neurosci 23:935–944
53. Curcio L, Podda MV, Leone L et al (2013) Reduced D-serine levels in the nucleus accumbens of cocaine-treated rats hinder the induction of NMDA receptor-dependent synaptic plasticity. Brain 136:1216–1230
54. Livak KJ, Schmittgen TD (2001) Analysis of relative gene expression data using real-time quantitative PCR and the 2(-Delta Delta C(T)). Methods 25:402–408
55. Fusco S, Ripoli C, Podda MV et al (2012) A role for neuronal CREB (cAMP responsive element binding)-1 in brain responses to calorie restriction. Proc Natl Acad Sci U S A 109:621–626
56. Gaudillière B, Konishi Y, de la Iglesia N et al (2004) A CaMKII-NeuroD signaling pathway specifies dendritic morphogenesis. Neuron 41:229–241
57. Ince-Dunn G, Hall BJ, Hu SC et al (2006) Regulation of thalamocortical patterning and synaptic maturation by NeuroD2. Neuron 49:683–695
58. Olson JM, Asakura A, Snider L et al (2001) NeuroD2 is necessary for development and survival of central nervous system neurons. Dev Biol 234:174–187
59. Pleasure SJ, Collins AE, Lowenstein DH (2000) Unique expression patterns of cell fate molecules delineate sequential stages of dentate gyrus development. J Neurosci 20:6095–6105
60. Di Lazzaro V, Capone F, Apollonio F et al (2013) A consensus panel review of central nervous system effects of the exposure to low-intensity extremely low-frequency magnetic fields. Brain Stimul 6:469–476
61. Machado S, Paes F, Velasques B et al (2012) Is rTMS an effective therapeutic strategy that can be used to treat anxiety disorders? Neuropharmacology 62:125–134

62. Hatakeyama J, Kageyama R (2004) Retinal cell fate determination and bHLH factors. Semin Cell Dev Biol 15:83–89
63. Ishibashi M, Ang SL, Shiota K et al (1995) Targeted disruption of mammalian hairy and enhancer of split homolog-1 (HES-1) leads to up-regulation of neural helix–loop–helix factors, premature neurogenesis, and severe neural tube defects. Genes Dev 9:3136–3148
64. Tomita K, Nakanishi S, Guillemot F et al (1996) Mash1 promotes neuronal differentiation in the retina. Genes Cells 1:765–774
65. Shimojo H, Ohtsuka T, Kageyama R (2011) Dynamic expression of Notch signaling genes in neural stem/progenitor cells. Front Neurosci 5:1–7
66. Zhou X, Smith AJ, Waterhouse A et al (2013) Hes1 desynchronizes differentiation of pluripotent cells by modulating STAT3 activity. Stem Cells 31:1511–1522
67. Fu J, Tay SS, Ling EA, Dheen ST (2006) High glucose alters the expression of genes involved in proliferation and cell-fate specification of embryonic neural stem cells. Diabetologia 49:1027–1038
68. Zhuang PW, Cui GZ, Zhang YJ et al (2013) Baicalin regulates neuronal fate decision in neural stem/progenitor cells and stimulates hippocampal neurogenesis in adult rats. CNS Neurosci Ther 19:154–162
69. Sinnegger-Brauns MJ, Huber IG, Koschak A et al (2009) Expression and 1,4-dihydropyridine-binding properties of brain L-type calcium channel isoforms. Mol Pharmacol 75:407–414
70. Morgado-Valle C, Verdugo-Díaz L, García DE et al (1998) The role of voltage-gated Ca^{2+} channels in neurite growth of cultured chromaffin cells induced by extremely low frequency (ELF) magnetic field stimulation. Cell Tissue Res 291:217–230
71. Olivares-Bañuelos T, Navarro L, González A et al (2004) Differentiation of chromaffin cells elicited by ELF MF modifies gene expression pattern. Cell Biol Int 28:273–279
72. Deisseroth K, Singla S, Toda H et al (2004) Excitation–neurogenesis coupling in adult neural stem/progenitor cells. Neuron 42:535–552
73. Ramírez M, Hernández-Montoya J, Sánchez-Serrano SL et al (2012) GABA-mediated induction of early neuronal markers expression in postnatal rat progenitor cells in culture. Neuroscience 224:210–222
74. West AE, Chen WG, Dalva MB et al (2001) Calcium regulation of neuronal gene expression. Proc Natl Acad Sci U S A 98:11024–11031
75. Jagasia R, Steib K, Englberger E et al (2009) GABA-cAMP response element-binding protein signaling regulates maturation and survival of newly generated neurons in the adult hippocampus. J Neurosci 29:7966–7977
76. Merz K, Herold S, Lie DC (2011) CREB in adult neurogenesis–master and partner in the development of adult-born neurons. Eur J Neurosci 33:1078–1086
77. Benito E, Barco A (2010) CREB's control of intrinsic and synaptic plasticity: implications for CREB-dependent memory models. Trends Neurosci 33:230–240
78. Bito H, Takemoto-Kimura S (2003) Ca(2+)/CREB/CBP-dependent gene regulation: a shared mechanism critical in long-term synaptic plasticity and neuronal survival. Cell Calcium 34:425–430
79. Wang J, Weaver IC, Gauthier-Fisher A et al (2010) CBP histone acetyltransferase activity regulates embryonic neural differentiation in the normal and Rubinstein–Taybi syndrome brain. Dev Cell 18:114–125
80. Min SW, Cho SH, Zhou Y et al (2010) Acetylation of tau inhibits its degradation and contributes to tauopathy. Neuron 67:953–966
81. Prozorovski T, Schulze-Topphoff U, Glumm R et al (2008) Sirt1 contributes critically to the redox-dependent fate of neural progenitors. Nat Cell Biol 10:385–394
82. Gaub P, Tedeschi A, Puttagunta R et al (2010) HDAC inhibition promotes neuronal outgrowth and counteracts growth cone collapse through CBP/p300 and P/CAF-dependent p53 acetylation. Cell Death Differ 17:1392–1408
83. Foti SB, Chou A, Moll AD et al (2013) HDAC inhibitors dysregulate neural stem cell activity in the postnatal mouse brain. Int J Dev Neurosci 31:434–447
84. Chatterjee S, Mizar P, Cassel R et al (2013) A novel activator of CBP/p300 acetyltransferases promotes neurogenesis and extends memory duration in adult mice. J Neurosci 33:10698–10712
85. Huang HY, Liu DD, Chang HF et al (2012) Histone deacetylase inhibition mediates urocortin-induced antiproliferation and neuronal differentiation in neural stem cells. Stem Cells 30:2760–2773
86. Yu IT, Park JY, Kim SH et al (2009) Valproic acid promotes neuronal differentiation by induction of proneural factors in association with H4 acetylation. Neuropharmacology 56:473–480
87. Shibasaki M, Mizuno K, Kurokawa K et al (2011) L-type voltage-dependent calcium channels facilitate acetylation of histone H3 through PKCγ phosphorylation in mice with methamphetamine-induced place preference. J Neurochem 118:1056–1066
88. Chen X, Lepier A, Berninger B et al (2012) Cultured subventricular zone progenitor cells transduced with neurogenin-2 become mature glutamatergic neurons and integrate into the dentate gyrus. PLoS ONE 7:e31547
89. Cho IS, Jung M, Kwon KS et al (2012) Deregulation of CREB signaling pathway induced by chronic hyperglycemia downregulates NeuroD transcription. PLoS ONE 7:e34860. doi:10.1371/journal.pone.0034860
90. Liu M, Pleasure SJ, Collins AE et al (2000) Loss of BETA2/NeuroD leads to malformation of the dentate gyrus and epilepsy. Proc Natl Acad Sci U S A 97:865–870
91. Fedele V, Roybon L, Nordström U et al (2011) Neurogenesis in the R6/2 mouse model of Huntington's disease is impaired at the level of NeuroD1. Neuroscience 173:76–81